JOURNAL OF MATERIALS SCIENCE 26 (1991) 1891–1898

# High temperature mechanical behaviour of an uncoated SiC–SiC composite material

M. GOMINA, P. FOURVEL, M.-H. ROUILLON
*LERMAT, ISMRa-Université, URA 1317, Boulevard du Maréchal Juin, 14050 Caen Cedex, France*

Flexural tests have been performed on unnotched specimens of an uncoated SiC–SiC laminar composite material to check the influence of specimen thickness and temperature (22 to 1200 °C in air) on the strength and the elastic modulus. An important modification of the loading curves and crack paths occurred when the temperature was increased, corresponding to a strengthening of the fibre–matrix interface.

## 1. Introduction

A great deal of effort has been devoted over the years to investigate new materials available for specific applications under high stress, high temperature or severe environment conditions, that is, for the new generation of diesel engines, rocket nozzles, or thermal protection parts of space shuttles. Today a few fibrous composite materials are available; the most promising of them are made of carbon or silicon carbide matrix. Kim *et al.* [1] evaluated the fracture toughness of a two-dimensional woven C–C laminate material by linear elastic fracture mechanics (LEFM), *R*-curve and *J* integral methods. They found only the *J* integral is an appropriate fracture mechanism parameter for this type of material. The stress intensity factors $K_{IC}$, $K_C$ and $K_Q$ from LEFM and the crack growth resistance $K_R$ were dependent on the orientation of the initial crack and on the value of $a/w$. Sakai et al. [2] investigated the fracture toughness anisotropy of a two-dimensional laminar SiC (Nicalon)–CVI–βSiC composite using three-point bending tests on chevron-notched specimens. They found that rising *R* curves for the cross-fabric orientation specimens are directly related to the fibre bridging of the newly created crack. The contribution of the wake region is shown to be an important factor to the toughening of these composites. Since these materials are destined to high-temperature utilizations, the question is whether the effects of the wake region will remain important; that is will a rising *R* curve be preserved. We intend to check these points in two steps for a SiC Nicalon–CVI–βSiC matrix composite. The first step which is the subject of the present paper is devoted to the evolutions of the fracture stress, elastic modulus, loading curves behaviour and fracture mechanisms with test temperature (22 to 1200 °C) and specimen depth. The second step will deal with fracture energy evaluations in a future paper.

## 2. Materials and specimens

### 2.1. Materials

This report concerns SiC–SiC materials in which the reinforcement is a two-directional isotropic tissue made of Nicalon SiC fibres. These so-called SiC fibres really contain SiC ( $\simeq$ 65 wt %) as aggregates and $SiO_2$ deeply present in the fibre. The oxygen is introduced at the beginning of the process when the starting polymer is treated at low temperature in air.

The matrix deposited using the CVI method is a β-SiC type of good mechanical quality [3]. The porosity is the third phase in this material ( $\simeq$ 15 vol %). Its size distribution, the localization and the orientation of the pores [4] have a great influence on the failure modes depending on the specimen orientation.

The material is designed to contain 35 vol % fibres with a final density between 2.4 to 2.6. Extensive descriptions of the materials are now available in the literature [5].

### 2.2. Specimens

Only [1, 3] orientation (usually called flatwise orientation) specimens were investigated. These specimens were from a specific experimental material, and they were not coated to prevent chemical reactions with the environment during the test. All the bending specimens were 70 mm long and 9.5 mm wide. Using a span of 60 mm, the span to depth ratios were 6.3 (thickness 9.5 mm with 23 laminates), 12 (thickness 5 mm with 16 laminates) and 24 (thickness 2.5 mm with 7 laminates).

## 3. Rupture tests

### 3.1. Testing method

Three-point bending tests were performed on a 1185 Instron machine at a cross-head speed of 20 μm $min^{-1}$, using a 10 kN load cell. The displacement of the load application point was measured under the upper knife from the signals of two linear variable differential transducers (LVDT), through alumina rods. These transducers were mounted symmetrically in respect to the loading axis, thus ensuring a good in-plane stability. The displacement signal used for recording the loading curve *P–h* was the mean value of the two signals from the transducers. For this experi-

0022–2461/91 $03.00 + .12 

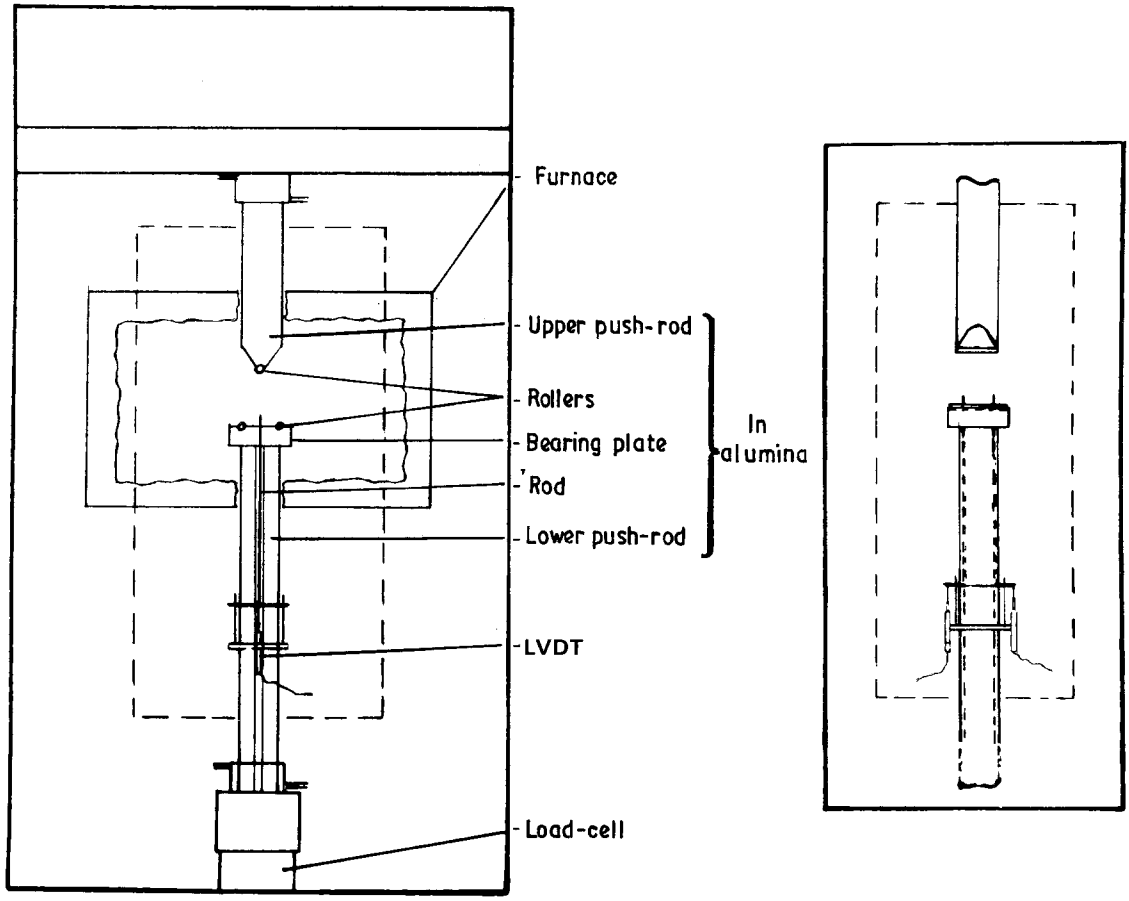


*Figure 1* Scheme of the three-point bending set used for testing SiC–SiC materials at high temperature in air.

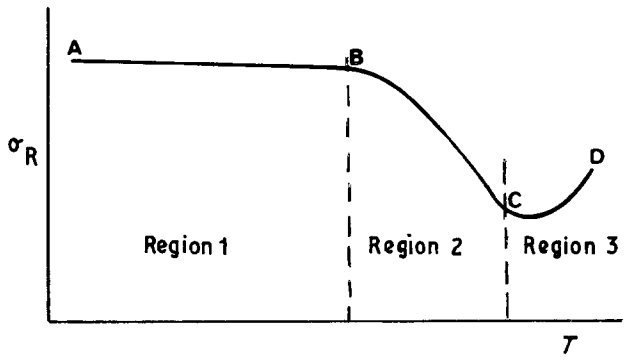


*Figure 2* General behaviour of the failure strength as a function of temperature for polycrystalline ceramics.

mental set to be designed for high temperature measurements, the push rods, the rollers and the bearing plates were made in polycrystalline alumina (AF 997, Desmarquest) and were permanently set in the heating system (Fig. 1).

## 3.2. Procedure

When testing the first type of SiC–SiC materials, we put the specimens in the furnance at room temperature (r.t.) and then heated them to the chosen test temperature ($T$). The consequences of this long exposure of the specimens to high temperature in air were a time effect and probably a deep oxidation effect. For the specimens investigated here, we put them in the furnace once the test temperature was reached. The excellent thermal shock resistance of the material allows this procedure which shortened the duration of exposure at high temperature.

## 3.3. Results and discussion

Measurements of the flexural strength and the elastic modulus of unnotched specimens were performed in order to check the influences of specimen thickness and temperature. These two parameters, when associated with the loading rate and duration, are very important for part survival predictions.

### *3.3.1. Flexural strength $\sigma_R$ and elastic modulus E*

*3.3.1.1. Temperature effects*

(a) Polycrystalline ceramics

The general behaviour of the failure strength as a function of temperature for fine polycrystalline ceramics is shown in Fig. 2 [6, 7]. This curve exhibits three regions:

(i) in region A–B the failure is due to the propagation of the pre-existing defects (from the process or inducted in service). This region corresponds to the brittle behaviour of the material,

(ii) in region B–C some plasticity appears; the failure behaviour moves from brittle to ductile. The rupture is governed by the intergranular phase or by the pores,

(iii) failure in region C–D is totally ductile and is

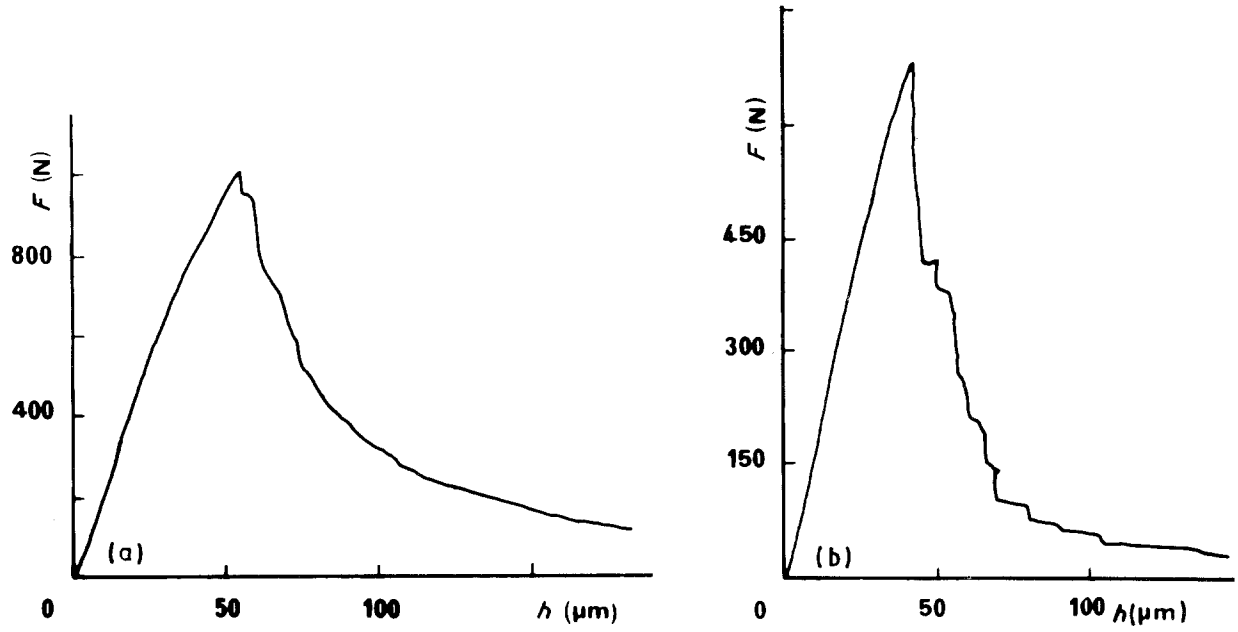


*Figure 3* Experimental flexural curves of unnotched SiC–SiC specimens of dimensions 70 × 9.5 × 5 mm$^3$, tested at (a) 22 °C and (b) 900 °C.

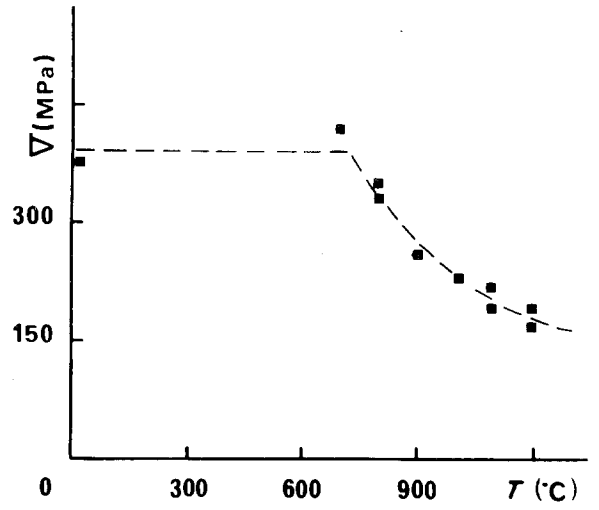


*Figure 4* Flexural strength determined by three-point bending in air, as a function of test temperature for SiC–SiC specimens of dimensions 70 × 9.5 × 5 mm$^3$.

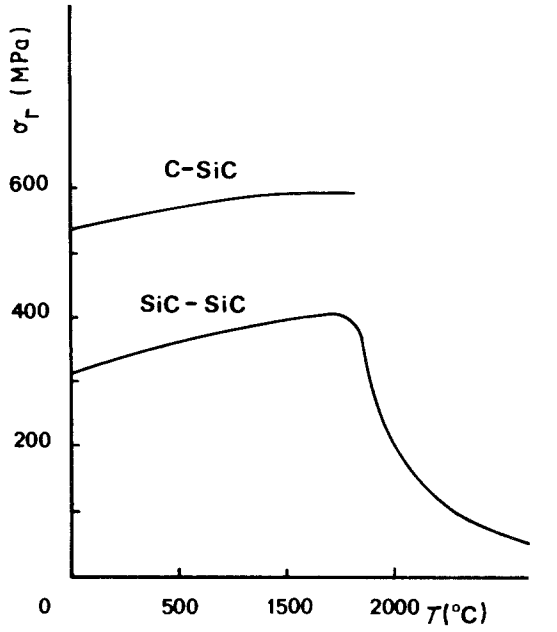


*Figure 5* Flexural strength of SiC–SiC and C–SiC materials as a function of test temperature in vacuum, according to Bernhart *et al.* [8].

governed by the yielding stress. Only a few materials exhibit such a behaviour.

(b) SiC–SiC Materials

Figs. 3a and 3b show the load against deflection curves for the 22 and 900 °C tests for SiC–SiC specimens of dimensions 70 × 9.5 × 5 mm$^3$ (depth 5 mm). The change in slope of the composite loading curves at approximately one-half of the maximum load represents the onset of fibre–matrix interface microcracking. This non-linearity is less pronounced at high temperature.

The maximum flexural tensile stress $\sigma_R$ was calculated at fracture using simple elastic beam theory and the resultant data are represented in Fig. 4 for the 70 × 9.5 × 5 mm$^3$ specimens. The strength at 22 °C is 380 MPa which slightly increased up to 420 MPa at 700 °C and then continuously drops off. This results looks very different from the one obtained by Bernhart *et al.* [8] when testing this material under vacuum (Fig. 5) or from a 45 vol % SiC (Nicalon)–SiC (CVI) material [9] tested in an Ar–$H_2$ atmosphere (Fig. 6).

This shows the effect of the atmosphere during the test: in our test conditions the oxidation of the carbonaceous fibre–matrix interface is responsible for the decreasing $\sigma_R$ value from temperature as low as 700 °C. This point will be discussed further from the optical and scanning electron microscope observations.

For the purpose of comparison, Fig. 7 shows the flexural stress as a function of temperature for the three groups of specimens studied. A common feature is the change in these curves at $T = 700$ °C related to the interphase oxidation.

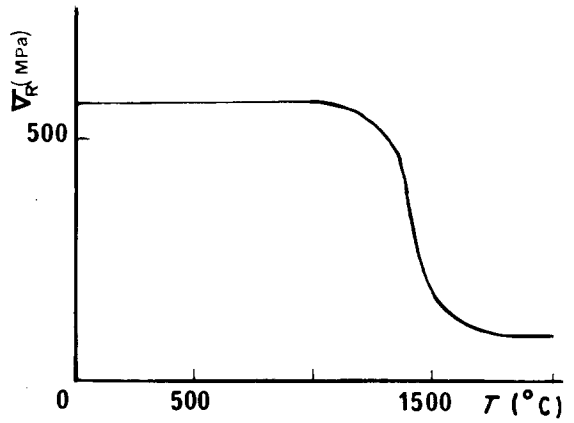


*Figure 6* Flexural strength of SiC–SiC materials determined by three-point bending, tested in an Ar–$H_2$ atmosphere as a function of test temperature for SiC–SiC specimens dimensions 70 × 9.5 × 5 mm$^3$ (according to Dauchier *et al.* [9].

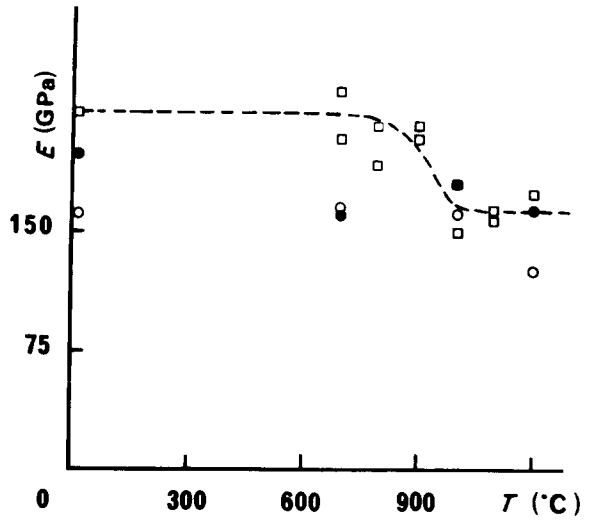


*Figure 8* Elastic modulus of SiC–SiC materials as a function of test temperature in air for three specimen depths. (□ 9.5 mm, ● 2.5 mm, ○ 5 mm)

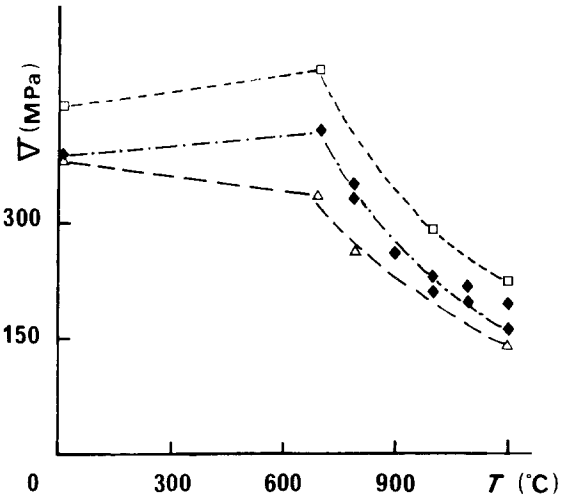


*Figure 7* Flexural strength of SiC–SiC materials as a function of test temperatures in air for the three specimens depths, *W*. (□ 9.5 mm, ◆ 5 mm, △ 2.5 mm).

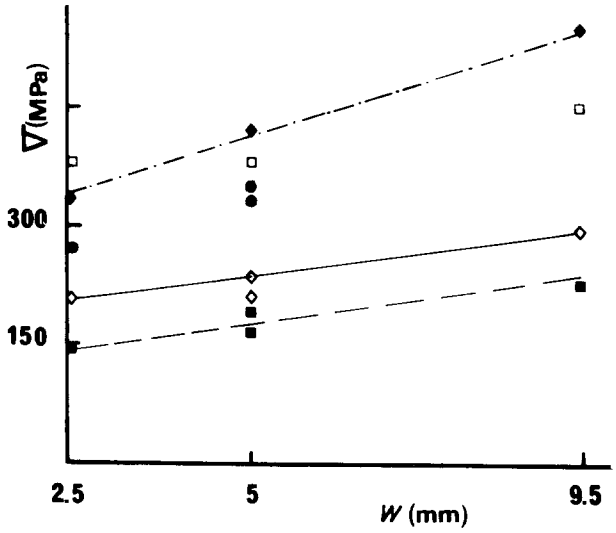


*Figure 9* Flexural strength of SiC–SiC materials as a function of specimen depth, for test temperatures in air. (□ 25 °C, ◆ 700 °C, ● 800 °C, ◇ 1000 °C, ■ 1200 °C).

The elastic modulus $E$ measured from the linear part of the load–deflection curve appears to be a slightly decreasing function of the test temperature (Fig. 8), although the measured values on thick specimens are to be taken with care. The initial value of 210 GPa at 22 °C for the composite (with dimensions 70 × 9.5 × 5 mm$^3$) is identical to the fibres' modulus and the decrease with temperature beyond 900 °C is due to a structural modification of the fibres or, more likely, to a not so good fibres–matrix adhesion.

*3.3.1.2. Interlaminar shear effects.* One of the problems attached to three-point bending tests is the evaluation of the shear stress $\tau$ which superimposes on the given tensile stress $\sigma$. When testing fine grain polycrystalline ceramics (SiC, $Al_2O_3$, $Si_3N_4$, . . . ), the effect of the shear stress is always negligible. In our tests the loading axis was normal to the isotropic plane of the tissue, that is the shear stress in the interlaminar layers acts in the weakest orientation (3, 1). The effect appears clearly when testing (1, 3) orientation notched specimens: the failure is delamination assisted. Then for unnotched specimens, the estimate of the flexural strength by the calculated theoretical tensile stress may be inappropriate, depending on the specimen depth for a given span, that is the shearing stress superimposes on the tensile stress to initiate cracks from the structural defects. The measured flexural stresses are reported in Fig. 9 as a function of specimens' depth $W$ (for a constant span of 60 mm) for five values of test temperature. The main points are as follows.

(i) At room temperature the flexural stress is unchanged from $W = 2.5$ to 5 mm depth, whereas the increase from $W = 5$ to 9.5 mm depth is due to a smaller interlaminar shear effect.

(ii) Except for the tests realized at 700 °C, the flexural stresses measured at high temperature are lower than those at 22 °C. This exception occurs from $W = 5$ mm and may be due to a modification of the fibre–matrix interface which results in a better contact

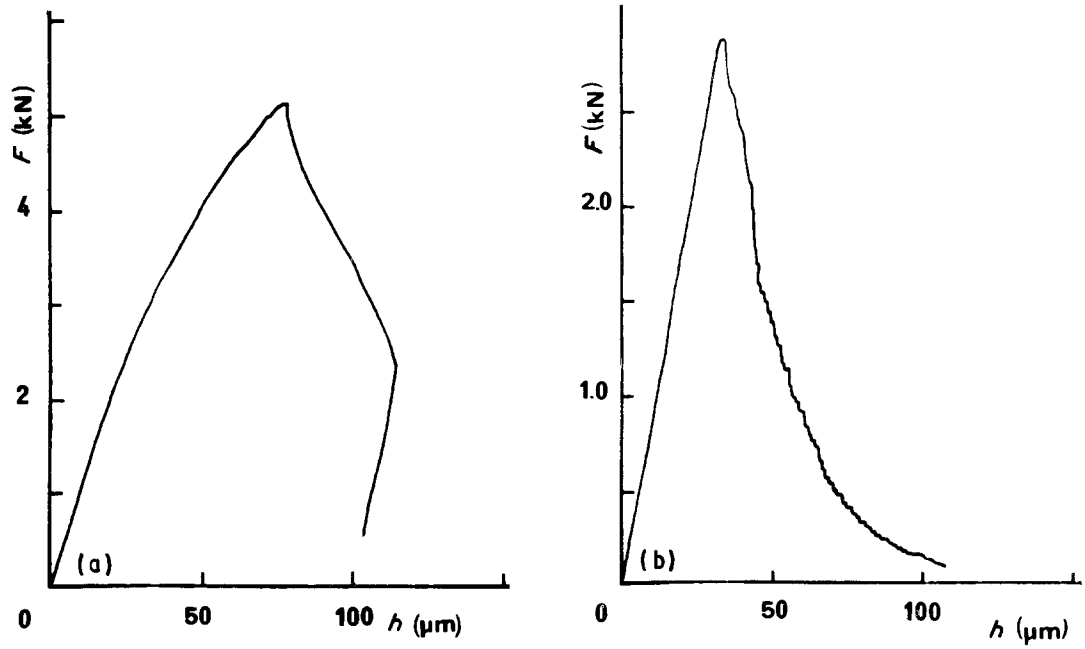


*Figure 10* Three point bending monotonic loading curves of SiC–SiC materials tested in air: a) non linearity before maximum load at 700 °C – b) total linearity at 1000 °C. (70 × 9.5 × 9.5 mm$^3$).

between these two phases. The tensile stress is then enhanced while the sliding of the fibres is lowered. This must appear in the scanning electron microscope observations.

(iii) At higher temperatures the flexural strength increases linearly with the specimen depth, that is the material becomes less sensitive to defects. This behaviour is the consequence of two oxidation effects: first the carbonaceous interface is destroyed and the friction becomes more important; the second effect is the embrittlement of the fibres, thus the entire material becomes brittle. Figs 10a and 10b show this embrittlement of this composite from 700 to 1000 °C.

Kromp *et al.* [10] have recently proposed a method for prediction of delamination in laminated specimens. The method is based on the elastic behaviour of each beam and it consists in measuring the ultimate shear stress $\tau^*$ and ultimate tensile stress $\sigma^*$. For a given specimen the $\Gamma$ value

$$\Gamma = \frac{\tau_{vert}}{\sigma_{xx}} = \frac{\Delta W}{W} \quad (1)$$

where $\sigma_{xx}$ is the tensile stress ahead of the notch, $\tau_{vert}$ is the normal shear stress, which is to be compared to $\Gamma^* = \tau^*/\sigma^*$. If $\Gamma < \Gamma^*$, the specimen failure will be governed by the tensile stress, whereas $\Gamma > \Gamma^*$ is the condition for delamination. For such an evaluation to be made for our SiC–SiC materials, (3, 1) orientation specimens need to be tested to check the $\tau^*$ value.

### 3.3.2. The effects of temperature on notched specimens

Before performing fracture toughness measurements and fracture energy evaluations we intended to check the effects of temperature on the loading curves (monotonical loading and loading–unloading).

(i) Figs 11a and 11b show an example of two monotonical loading curves obtained with 5 mm depth specimens with a relative notch length $a_0/W = 0.4$ tested at 22 and 1000 °C. Increasing temperature reduces the deformation before the maximum load and also the total deformation. Another effect is the discontinuous rupture of the material which supports the idea of an embrittlement of the fibre bundle.

We have reported in Fig. 12 the maximum load values as a function of the test temperatures. It appears that there is a linear decreasing relation which we can relate to linear fracture mechanics concepts

$$K_{IC} = \frac{3}{2}\frac{FL}{BW^2}Ya^{1/2} \quad (2)$$

or

$$F = \frac{K_{IC}}{Ya^{1/2}}\frac{2BW^2}{3L} \quad (3)$$

The linear relation from Fig. 12 is

$$F(T) = F(rt) - \alpha T$$

and then

$$K_{IC} = K_{I0} - f(T) \quad (4)$$

It is worth studying this relation more carefully using other specimen depths as it may provide a way to predict $K_{IC}$ dependence on temperature.

(ii) Observation of loading–unloading curves confirms the reduction in deformation when increasing test temperature. It also appears that inside a loading–unloading loop a significant drop of the load may occur. This corresponds to the breakage of fibres and the crack is further deflected by the pores (Fig. 13). The fracture energy measurements must be sensitive to this modification in the failure mode.

### 3.3.3. Optical and scanning electron microscope observations

Only the unnotched specimens were concerned with these primary observations made on polished surfaces

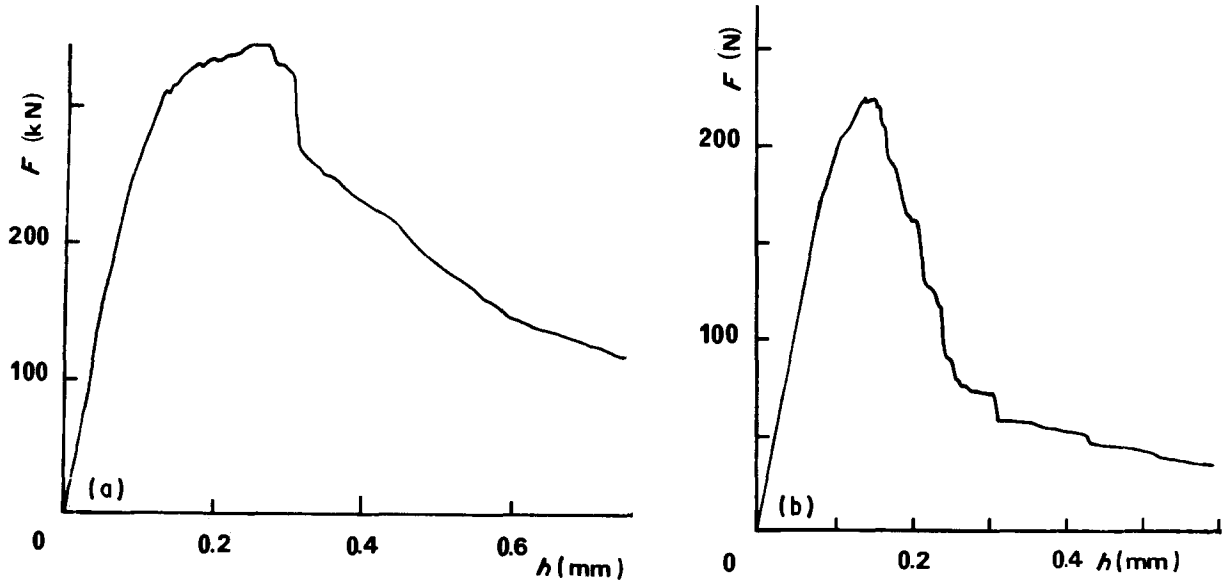


*Figure 11* Three point bending monotonical loading curves of notched SiC–SiC specimens: a) $T = 22\,°C$; b) $T = 1000\,°C$. ($70 \times 9.5 \times 5\ mm^3$).

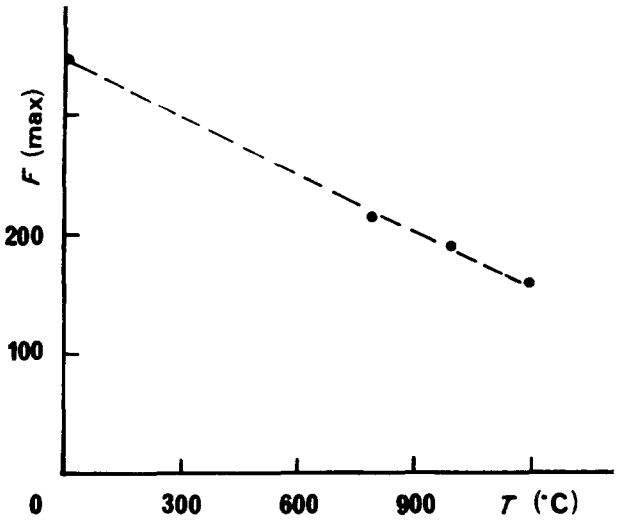


*Figure 12* Maximum load values measured on notched SiC–SiC specimens as a function of test temperatures. ($70 \times 9.5 \times 5\ mm^3$).

and on the surfaces of rupture. The main features are as follows.

(i) Whatever the specimen depth, at room temperature the crack is strongly deflected from the tensile face to the upper side and optical observations inside the crack confirm the presence of fibres bridging the crack mouth. Moreover, optical observations reveal there is a unique crack at the starting point which first propagates under the action of the tensile stress and then is further submitted to the shear stress. The point of maximum deviation lies in the horizontal mid-plane. Scanning electron microscope observations show a large extent of fibre pull-out (pull-out lengths > 100 μm are observed) from the bundles normal to the crack plane (Fig. 14a), whereas the fibres in the other direction debond from the matrix (Fig. 14b). On the debonded lengths, the fibre surface is free of any matrix but the embedded part is strongly bonded to the matrix. The surfaces of rupture are covered by the debris of the SiC matrix (Fig. 14c).

(ii) At higher temperatures (beyond 800 °C) the crack propagation in a straight line means that the fibre–matrix interface is stronger. The absence of non-linearity on the loading curve corroborates the idea that the modified interface is no longer favourable to fibre sliding. No crack mouth bridging is thus observed and scanning electron microscope images show brittle rupture of the fibres (Fig. 14d). Only a little

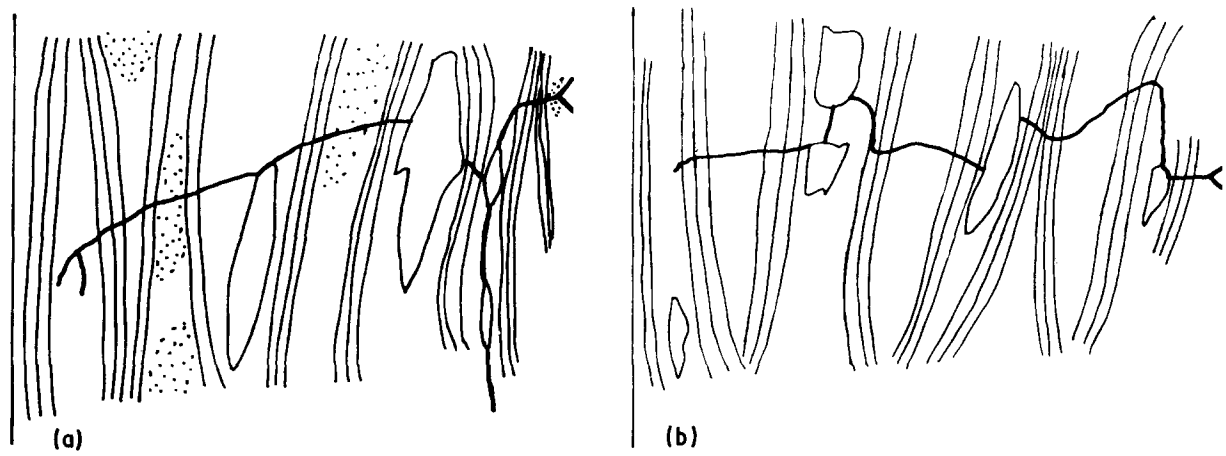


*Figure 13* Crack paths observed on polished surfaces: (a) specimen tested at 800 °C, (b) specimen tested at 1000 °C.

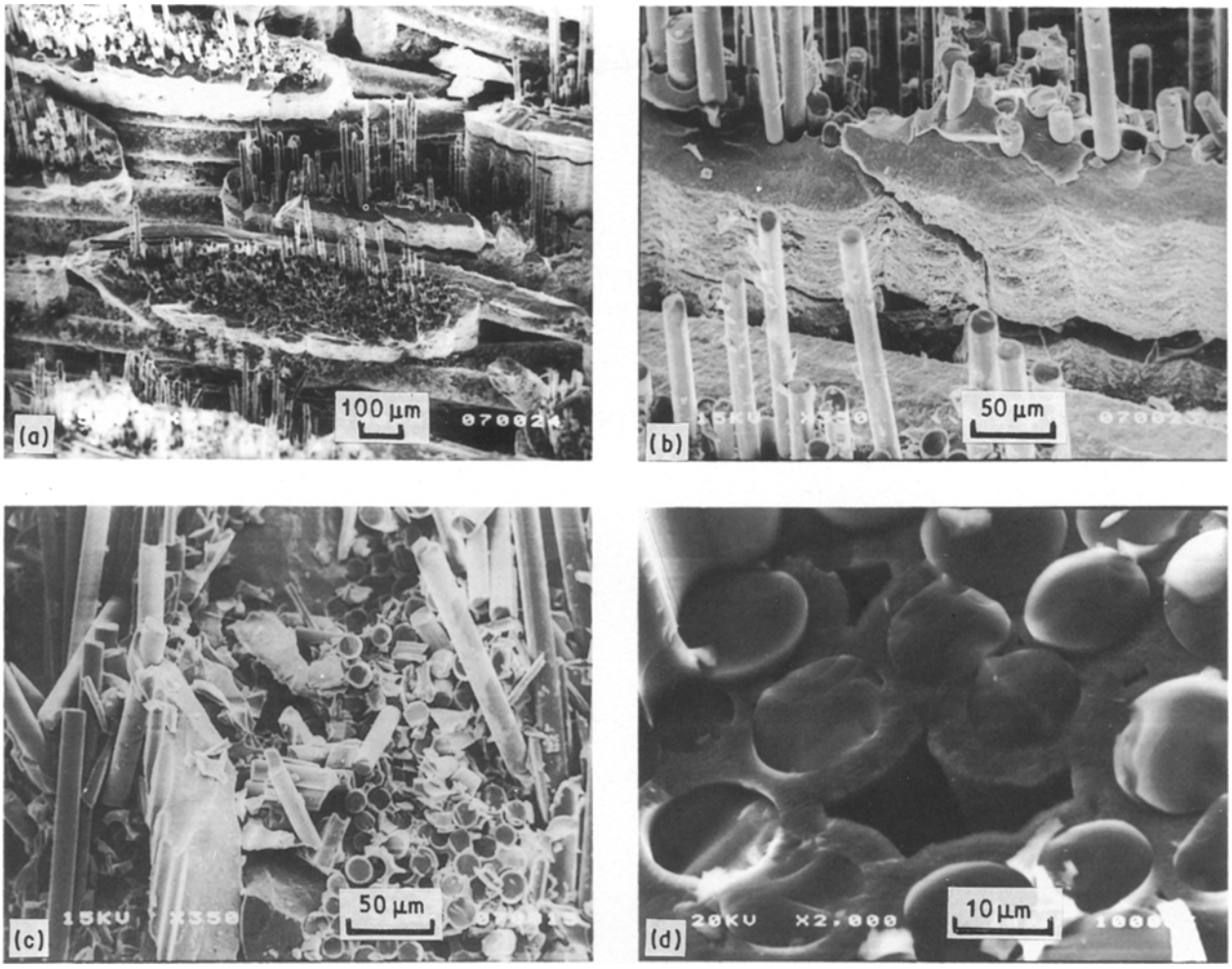


*Figure 14* Scanning electron micrographs of the rupture surfaces of SiC–SiC composites.

debris of the SiC matrix is observable on the surfaces of rupture. As a consequence of the intimate adhesion of the matrix to the fibres, when pull-out is effective, the fibre lengths are very short.

The proposed sequence of the material failures are the following.

(i) At relatively low temperatures (from room temperature to 700–800 °C), in a first stage the specimen deforms elastically due to the progressive loading of the fibres (the measured composite modulus corresponds to the fibre modulus). The non-linear part of the $P$–$h$ curve should correspond to the sliding of fibres in the matrix and to the matrix cracking. Ahead of the crack, the matrix fails first and the breakage of fibres results in instability points on the $P$–$h$ curve.

(ii) At higher temperatures the main feature is the interface modification in air (it grows hard) which prevents the fibres sliding. This results in less important total deformation and residual displacements. It is not yet clear whether the brittle rupture of the fibres at high temperature is due to a structural evolution or is a consequence of the interface hardening.

## 4. Conclusions

There is an evolution in the failure mode of SiC–SiC materials with test temperature. From room temperature to 700 °C the rupture sequence is controlled by the fibre–matrix interface, the flexural strength increases while the elastic modulus is unchanged. The surfaces of rupture exhibit long pull-out lengths and a lot of matrix debris.

The SiC matrix is first destroyed and then the fibres break under shear and tensile stresses. Beyond 700 °C, the flexural strength increases monotonically with the specimen depth and the failure mode changes to exhibit a brittle rupture of the fibres. The behaviour of this material will next be quantified through crack propagation energy values measured on notched specimens in future experiments.

## Acknowledgements

Part of this work has been supported by the European Economic Communities under BRITE Program (Contract P n°-1348-6-85) entitled "Reliability Thermomechanical and Fatigue Behaviour of High Temperature Structual Fibrous Ceramic Composites". The authors thank MM Lamicq, Bourgeon, Chateigner and Jouin from SEP (Bordeaux) for their helpful suggestions and advice.

## References

1. H. C. PAN, M. SAKAI, J. W. WARREN and R. C. BRADT, Tailoring Multiphase and Composite Ceramics, The Pennsylvania State University, University Park, Penn., USA July 17–19, 1985; edited by R. E. Tressler, G. L. Messing, C. G. Pantano and R. E. Newham, (Plenum, New York, 1986) pp. 20, 615.

2. H. C. KIM, K. J. YOON, R. PICKERING and P. J. SHERWOOD, *J. Mater. Sci.* **20** (1985) 3967.
3. G. A. BERNHART, Private communication.
4. M. GOMINA, J. L. CHERMANT and M. COSTER, *Acta Stereol.* **2** Suppl. 1 (1983) 179.
5. P. LAMICQ, G. A. BERNHART, M. M. DAUCHIER and J. G. MACE, *Amer. Ceram. Soc. Bull.* **64** (1985) 298.
6. R. W. DAVIDGE, "Mechanical Behaviour of Ceramics" (Cambridge University Press, Cambridge, 1979).
7. J. C. GLANDUS, PhD Thesis, Université de Limoges, Limoges (1981).
8. G. BERNHART, P. LAMICQ and J. MACE, *Ind. Céram.* **1/85** (1985) 790.
9. M. DAUCHIER, P. LAMICQ and J. MACE, *Rev. Int. Htes Temp. Réfract.* **19** (1982) 285.
10. K. KROMP, Communication at the Festigkeitsseminar, Keramische Werkstoffe und Metall-Keramik-Verbindungen, November 17–18 in Stuttgart 1986.

*Received 6 October 1989*
*and accepted 9 April 1990*